Photoelectrochemical Behavior of Oxalate at an Indium Tin Oxide Electrode

Natalia C. Tansil, Hong Xie, and Zhiqiang Gao*

Institute of Bioengineering and Nanotechnology, 31 Biopolis Way, Singapore 138669, Republic of Singapore

Received: June 22, 2004; In Final Form: August 19, 2004

The photoelectrochemical characteristics of oxalate in 0.20 M NaS_2O_4 at an indium tin oxide (ITO) electrode were investigated. Significant photocurrents were observed upon illumination in both the UV and visible regions with the highest photocurrent at 290 nm. The photocurrent onset was at ~−0.30 V (vs Ag/AgCl), and it increased linearly with an increase in illumination intensity, indicating that the charge carrier generation process is the limiting factor of the photocurrent generation at the ITO electrode. Deposition of a bovine serum albumin (BSA) monolayer on the ITO electrode surface suppressed the photocurrent, whereas the introduction of a second layer of $Ru(bpy)_3^{2+}$ (bpy = 2,2′-bipyridine) restored most of the photoelectrochemical response with a photocurrent action spectrum identical to that observed at the ITO electrode, suggesting that the $Ru(bpy)_3^{2+}$ layer promotes charge transfer between oxalate and the ITO electrode, but $Ru(bpy)_3^{2+}$ itself has little if any photoelectrochemical response in the system.

Introduction

Over the past few decades, there have been significant advances in the development of photoelectrochemical cells based on the immobilization of a photosensitizer layer onto a metal oxide semiconductor thin film.[1−3] Various photosensitizers, including organic,[4,5] inorganic,[1−3,6,7] and polymeric[8,9] dyes, have been reported. Among them, the family of ruthenium−bipyridine complexes has attracted greater attention.[1−3,6] On the other hand, most of the work on the semiconductor thin films has focused on TiO_2, SnO_2, and their composites with other metal oxides.[1−8] As demonstrated by O'Regan and Grätzel, a $Ru(bpy)_3^{2+}$-sensitized TiO_2 thin film based photoelectrochemical cell had a 15% solar to electric energy conversion efficiency and >80% incident monochromatic photon to current efficiency.[6] More recently, there has been interest in the use of photocurrent as an analytical signal for sensitive detection of biological affinity events.[10,11] One approach of producing an analyte-responsive photocurrent involves labeling one of the bioaffinitive species with a $Ru(bpy)_3^{2+}$ derivative as the photosensitizing tag, oxalate as the sacrificial electron donor [$Ru(bpy)_3^{2+}$−oxalate], and a nanoparticulate SnO_2 film coated indium tin oxide (ITO) electrode as the photocurrent collector.[10] The photosensitive $Ru(bpy)_3^{2+}$ tag is expected to impart a photoelectrochemical response upon illumination. It is suggested that the photoelectrochemical detection technique has the potential to match the high sensitivity of electrochemiluminescence. However, the contribution of the photocurrent of oxalate at the ITO substrate electrode to the total photoelectrochemical response of the system must be considered. To determine this contribution, we have studied the photoelectrochemistry of oxalate at the ITO electrode. Strong photoelectrochemical response was found in oxalate solution at the ITO electrode, instead of the $Ru(bpy)_3^{2+}$−oxalate at the nanoparticulate SnO_2 film coated ITO electrode. The need for caution in attributing the photocurrent or the photoelectrochemical properties to $Ru(bpy)_3^{2+}$ and its derivatives was emphasized.

* To whom correspondence should be addressed. Phone: +6824-7113. Fax: +6478-9080. E-mail: zqgao@ibn.a-star.edu.sg.

Experimental Section

Materials. Oxalic acid (>99%), $Ru(bpy)_3Cl_2$ (>99%), sodium oxalate (>99.5%), and bovine serum albumin (BSA; lyophilized power) were purchased from Sigma-Aldrich (St. Louis, MO). ITO-coated glass slides were from Delta Technologies Limited (Stillwater, MN). Conducting epoxy was purchased form Ladd Research (Williston, VT). All other reagents were obtained from Sigma-Aldrich and used without further purification. A 0.20 M Na_2SO_4 solution was used as the supporting electrolyte. The pH of the oxalate solution was controlled by adjusting the ratio of oxalic acid and sodium oxalate. All solutions were freshly prepared with deionized Milli-Q water of conductivity ≤18.2 MΩ cm (Millipore Corp., Billerica, MA). Oxygen gas was used for oxygenating and ultrapure argon gas was used for deoxygenating oxalate solutions.

Apparatus. Measurements of photocurrent and open-circuit photopotential were carried out using a CH Instruments model 660A electrochemical workstation (CH Instruments, Austin, TX). The three-electrode system consisted of the ITO working electrode, a nonleak miniature Ag/AgCl reference electrode (Cypress Systems, Lawrence, KS), and a platinum foil counter electrode. The ITO electrode was etched with an aqueous solution of 20% HCl and 5% HNO_3 except for the area of 0.20 cm^2 used as the working electrode. Electrical contact was made to the ITO electrode using conducting epoxy and a copper wire. The contact formed had a resistance of <1.0 Ω. The three electrodes were hosted in a standard fluorescence cuvette and arranged in such a way that the ITO electrode faces the illumination window and the other two electrodes are behind the ITO electrode and above the illumination pathway. BSA-coated ITO electrodes were prepared by soaking the ITO electrodes in 1.0 mg/mL BSA in phosphate-buffered saline (PBS) solution overnight. After adsorption, the electrodes were copiously rinsed with PBS, soaked in vigorously stirred PBS for 10 min, rinsed again, and blown dry with a stream of air. Introduction of $Ru(bpy)_3^{2+}$ to the BSA film was done through electrostatic interaction by soaking the BSA-coated electrode in 5.0 mg/mL $Ru(bpy)_3Cl_2$ in PBS for 10 min. Unreacted $Ru(bpy)_3Cl_2$ molecules were rinsed off by immersing them in

10.1021/jp047290g CCC: $27.50
Published on Web 10/06/2004

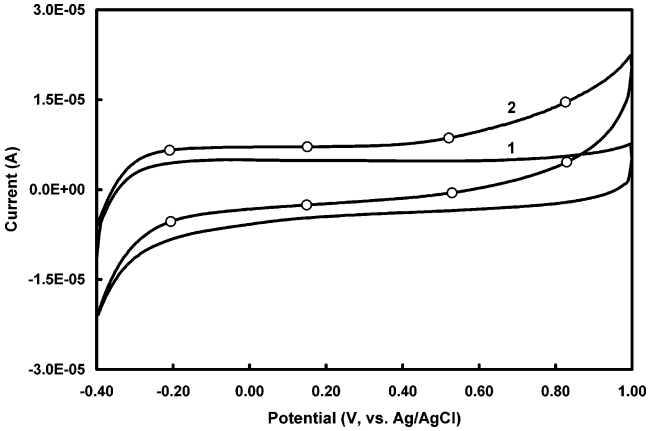

Figure 1. Cyclic voltammograms of oxalate at the ITO electrode (1) in the dark and (2) under illumination at 300 nm (10 mM oxalate in 0.20 M Na_2SO_4, potential scan rate 100 mV/s).

50 mL of PBS under vigorous stirring for 5 min. Illumination was performed with a Fluorolog-3 spectrofluorometer (Jobin Yvon Inc., Edison, NJ). The discovery mode of the spectrofluorometer was adopted for photocurrent action experiments at a 10 nm interval. The intensity of the monochromatic light incident on the ITO electrode was controlled by adjusting both the slit width and the distance to the illuminator, and was measured at $\lambda = 300$ nm using ferrioxalate actinometry.[12] Illumination was performed from the front of the ITO electrode to prevent the absorption of light by the glass substrate. All potentials reported in this work were referred to the Ag/AgCl electrode. All experiments were conducted at room temperature.

Results and Discussion

Photoelectrochemical Characteristics of Oxalate at the ITO Electrode. The voltammetric responses of oxalate at the ITO electrode in the dark and under illumination at 300 nm were first explored, and the cyclic voltammograms are shown in Figure 1. To avoid complications from the redox reactions of dissolved oxygen and oxalate, cyclic voltammetry was conducted in the range of -0.40 to $+1.0$ V. There was a substantial difference between the responses of oxalate at the ITO electrode in the dark and under illumination (Figure 1). Cathodic currents were observed at potentials more negative than -0.30 V under both dark and illumination conditions, evidently due to the electrochemical reduction of dissolved oxygen at the ITO electrode. The current observed between -0.20 and $+0.80$ V in the dark was mainly capacitive, and it was not much different from that of the supporting electrolyte. Upon illumination, a significant increase in the photocurrent was observed throughout the potential window. Moreover, the photocurrent was potential dependent; it increased as the applied potential was scanned toward more positive potential, particularly at potentials >0.30 V. Increased charge separation and the facile transport of charge carriers under positive bias are responsible for the enhanced photocurrent. The steep rise in the current at potentials beyond 0.90 V is probably due to the implication of direct oxidation of oxalate. It is well-known that, as an n-type semiconductor, the photoelectrochemical process of the ITO electrode is based on preferential hole injection into the electrolyte.[13,14] The application of a positive bias to the ITO electrode provides the necessary energy gradient to drive away the photogenerated holes and electrons in different directions, minimizes charge recombination, and therefore increases the photoelectrochemical efficiency.

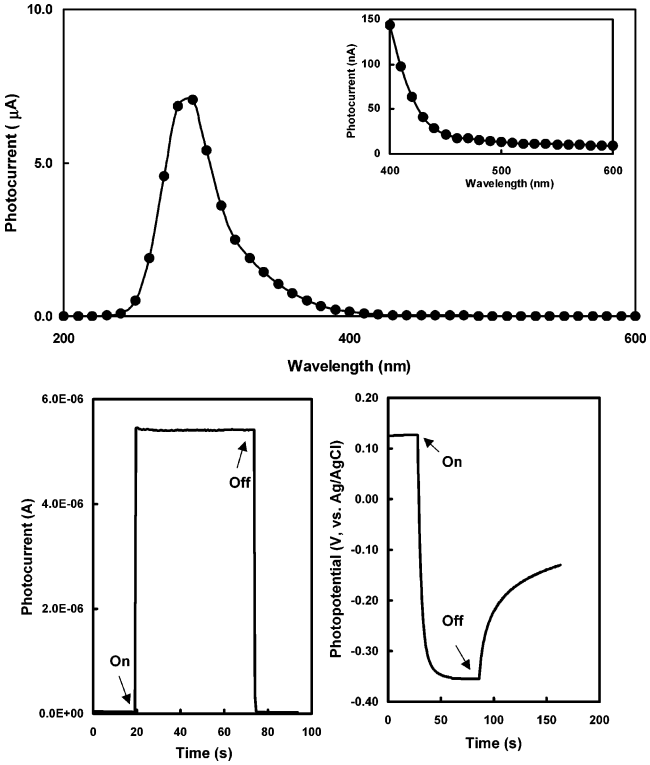

Figure 2. (A, top) Photocurrent action spectra of oxalate at the ITO electrode. The inset shows the photocurrent action spectrum in the visible region. Illumination was conducted with monochromatic light at a 10 nm interval. (B, bottom left) Photocurrent−time characteristics of oxalate at the ITO electrode during illumination. (C, bottom right) Open-circuit photopotential−time characteristics of oxalate at the ITO electrode during illumination. Conditions: 50 mM oxalate in 0.20 M Na_2SO_4, illumination conducted with monochromatic light of 300 nm, photocurrent collected at 0.30 V.

Photocurrent action spectra, i.e., plots of the observed photocurrent as a function of the wavelength of the incident light are shown in Figure 2A. The inset in Figure 2A is the magnified version of the action spectrum in the visible region. Photocurrents were observed upon illumination at wavelengths from 240 to 600 nm with the highest photocurrent of 7.0 μA at 290 nm. As shown in the inset in Figure 2A, significant photocurrent was also obtained at 470 nm, the wavelength used in Dong's experiments.[10] Parts B and C of Figure 2 illustrate the time dependence of the photocurrent and photopotential at the ITO electrode upon illumination. The rise and fall of the photocurrent and photopotential corresponded well to the illumination being switched on and off. As demonstrated in Figure 2B, the photocurrent generation consisted of two steps. The major fraction of the photocurrent appeared promptly after the illumination, followed by a slow decay (at low oxalate concentration), or a steady state (at high oxalate concentration). It took $\sim$1.0 s for the photocurrent to reach steady state. This pattern of photocurrent was highly reproducible for numerous on−off cycles of illumination. On the other hand, the photopotential response under open-circuit conditions was rather slow, as the photopotential continued to grow for as long as 60 s following the illumination (Figure 2C). This is indicative of the long time needed for the equilibrium to be established at the ITO electrode. The electrons that are transferred from oxalate into the ITO layer are likely to occupy shallow and deep traps. The slow growth in the photopotential observed in Figure 2C is likely to be influenced by such trap-filling phenomena.[15] Similar photoelectrochemical characteristics have previously been noted in nanostructured thin film based photoelectrochemi-

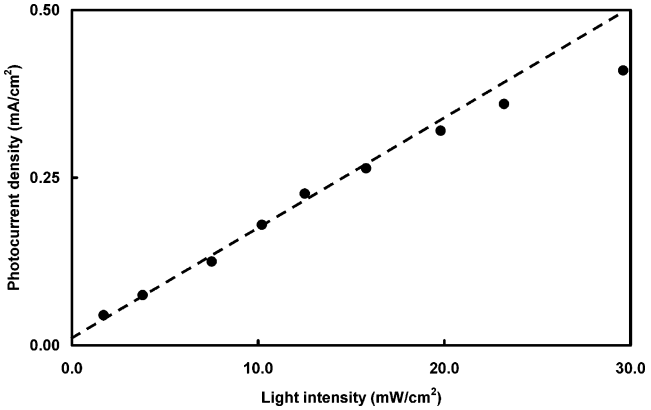

Figure 3. Dependence of photocurrent on the incident light intensity (50 mM oxalate in 0.20 M Na_2SO_4, illumination conducted with monochromatic light of 300 nm, photocurrent collected at 0.30 V).

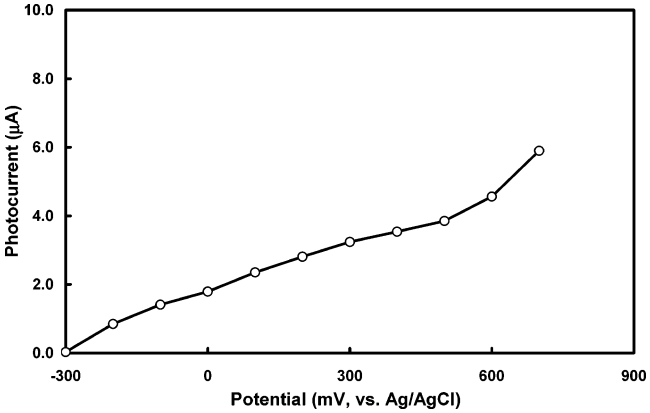

Figure 4. Dependence of photocurrent on the applied potential (20 mM oxalate in 0.20 M Na_2SO_4, illumination conducted with monochromatic light of 300 nm).

cal cells.[16,17] The photopotential reached a limiting value of −0.355 V, which is close to the redox potential of dissolved oxygen at the ITO electrode (Figure 1), implying that oxygen might be involved in the photoelectrochemical process of oxalate. A detailed study of the effect of dissolved oxygen on the photoelectrochemical process of oxalate revealed that little difference in photocurrent existed between oxygen-free oxalate solution (argon-purged for 30 min) and oxygen-containing oxalate solution (oxygen-purged for 30 min). Later experiments conducted at low oxalate concentrations showed that dissolved oxygen is, however, involved in scavenging photogenerated charge carriers, competing with oxalate for the photogenerated charge carriers. It has been pointed out that the amount of charge separation at the semiconductor/electrolyte interface is controlled by the redox couple and the band energies of the semiconductor, which, in turn, determines the potential difference achieved under illumination.[13] In this case, the dissolved oxygen plays an important role in determining the equilibrium photopotential.

Effect of Illumination Intensity. As expected the illumination intensity had a profound effect on the photocurrent. In this experiment, the light intensity was varied by adjusting the slit width of the spectrofluorometer and the distance to the illuminator. As illustrated in Figure 3, the photocurrent increased linearly with the incident light intensity up to 20 mW/cm^2 and gradually leveled off at higher intensity. The linear relationship between photocurrent and incident light intensity suggests that the photogeneration of charge carriers is a monophotonic process.[18] A quantitative measure of the photoelectrochemical properties is the incident photon to current efficiency (IPCE). The IPCE is the quantum yield for the production of majority charge carriers. It can be estimated by the following equation:[19]

$$\mathrm{IPCE} = (I_\lambda hc)/(W_\lambda \lambda e) \qquad (1)$$

where I_λ is the photocurrent, h the Planck constant, c the speed of light, W_λ the intensity of the incident light, λ the illumination wavelength, and e the electric charge of an electron. The IPCE value of oxalate at the ITO electrode was found to be in the range of 0.09−2.8%.

Effect of Applied Potential. Figure 4 depicts the dependence of photocurrent on the applied potential. As seen in Figure 4, the photocurrent increased gradually with the applied potential. The increase in photocurrent with positive bias is due to better charge collection efficiency, as the photogenerated charge carriers are more efficiently transported to the electrode. This is consistent with the trend observed in cyclic voltammetry. A similar dependence of photocurrent on applied potential has been observed in other thin film based photoelectrochemical systems.[19,20] The onset potential was found to be ∼−0.30 V. Below the onset potential, all photogenerated charge carriers recombine or are lost in interfacial reactions. As the applied potential increases, the fraction of lost electrons decreases. This fraction is practically independent of light intensity, implying that the photocurrent is only limited by the efficiency with which the electrons are transported to or withdrawn from the electrode.

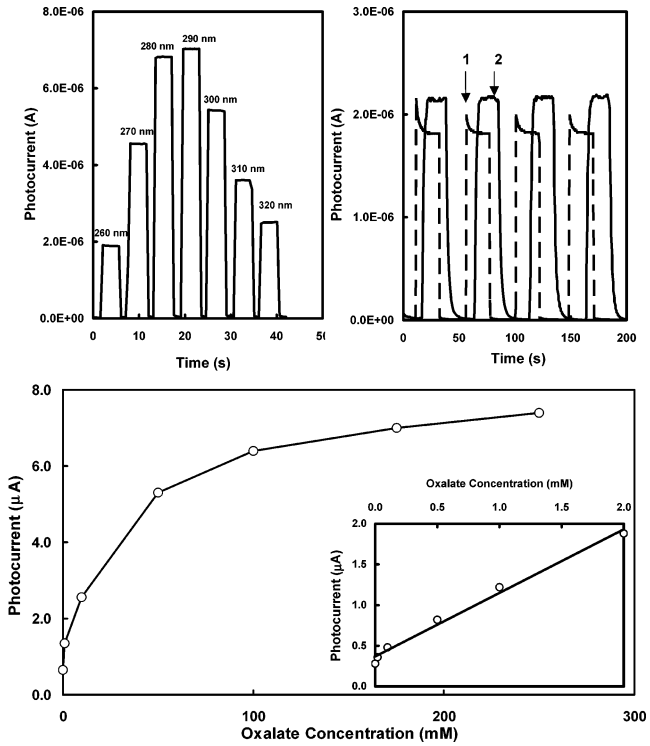

Figure 5. (A, top left) Photocurrent action spectrum of 100 mM oxalate between 260 and 320 nm. (B, top right) Photocurrent−time behavior of (1) 2.0 mM oxalate containing dissolved oxygen and (2) 2.0 mM oxygen-free oxalate. (C, bottom) Dependence of photocurrent on oxalate concentration. The inset shows the photocurrent−oxalate concentration relationship in the range of 0−2.0 mM. Conditions are as for Figure 2.

Dependence of Photocurrent on Oxalate Concentration. The photocurrent−time behavior of the ITO electrode in the presence of various concentrations of oxalate is shown in Figure 5A,B. At high concentration steady-state photocurrents were attained immediately after the light was switched on (Figure 5A). As depicted in Figure 5C, the steady-state photocurrent was directly proportional to the concentration of oxalate from

0.05 to 2.0 mM, indicating that the rate of oxalate oxidation at the ITO electrode is first order with respect to oxalate up to 2.0 mM. The increase in photocurrent started to level off at higher concentrations of oxalate, whereas at low concentrations an initial surge of the photocurrent followed by a quick decay was observed at wavelengths <400 nm after the light was switched on (Figure 5B, trace 1). It is unlikely that the photocurrent spike observed at low oxalate concentrations is caused by hole−electron separation at a space charge region of an n-type semiconductor electrode for the following reasons: It is oxalate concentration dependent, the decay time is measured in tens of seconds rather than milliseconds, and a cathodic photocurrent spike is not observed when the light is switched off.[21] The photocurrent decay at low concentrations of oxalate can presumably be explained as the following: Prior to illumination, oxalate ions are in equilibrium with the ITO electrode with some degree of penetration into the ITO film, and a higher concentration may be found at the electrode surface because of adsorption. Upon illumination, oxalate ions are rapidly oxidized by photogenerated holes at the electrode surface while photogenerated electrons are quickly collected by the electrode, giving an initial surge of the photocurrent. The oxalate concentration within the photoelectrochemical region is therefore depleted, and the dissolved oxygen begins to compete for the photogenerated charge carriers. The photogenerated charge carriers must now pass through a region of ultralow concentration of oxalate and high concentrations of surface-trapped holes and oxygen. Both surface-trapped holes and oxygen scavenge conduction band electrons. As a result, a significant amount of charge carriers are lost, hence the decay of the photocurrent. As anticipated, the oxygen effect was the most pronounced in the first on−off cycle (Figure 5B, trace 1). The role of dissolved oxygen in the photoelectrochemical process was further studied in an oxygen-free oxalate solution. The disappearance of the initial current spikes and the increase in photocurrent confirmed that oxygen in the solution does compete with oxalate for the photogenerated charge carriers (Figure 5B, trace 2). At high oxalate concentration, more than a sufficient amount of oxalate is always available in that region and a steady-state photocurrent is obtained.

Effect of a Coating on the ITO Electrode. Treatment of the ITO electrode in 1.0 mg/mL BSA solution resulted in the formation of a BSA monolayer on the electrode surface. As illustrated in trace 1 in Figure 6, much lower photocurrents were observed at the BSA-monolayer-coated electrode as compared to the bare ITO electrode, indicating that the monolayer impedes charge transfer between the ITO electrode and oxalate in solution. The photocurrent, which is mainly caused by charge transfer through the defects of the BSA monolayer, was significantly reduced by more than 80%. On the other hand, since $Ru(bpy)_3Cl_2$ is cationic and the BSA monolayer is anionic at pH 7.4, a brief soaking of the BSA-coated ITO electrode in 5.0 mg/mL $Ru(bpy)_3Cl_2$ solution resulted in the formation of a BSA/$Ru(bpy)_3^{2+}$ bilayer on the electrode via the layer-by-layer electrostatic self-assembly.[22−26] Subsequent photoelectrochemical tests in oxalate solution showed a photocurrent action spectrum essentially identical to that obtained at the bare ITO electrode, but with a ∼30% drop in the magnitude of the photocurrent throughout the wavelength range of 240−600 nm (Figure 6, trace 2). The photocurrent generated at 470 nm was comparable to that reported in ref 10 and 10−100-fold higher than that observed in ref 11. These changes are obviously attributed to the decrease in the electron tunneling pathway owing to the formation of the BSA/$Ru(bpy)_3^{2+}$ bilayer that

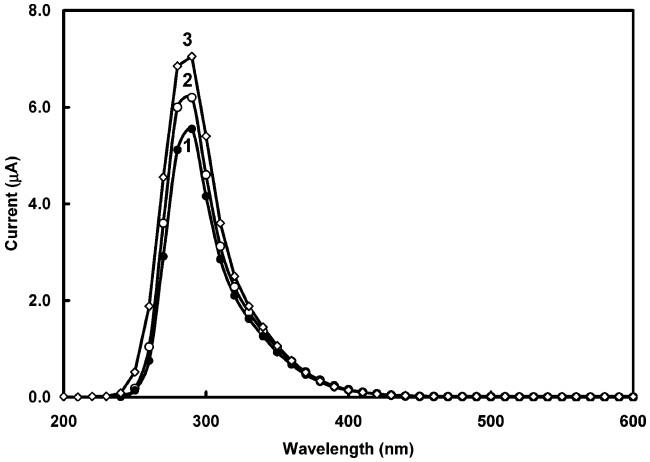

Figure 6. Photocurrent action spectra of oxalate at (1) the BSA monolayer, (2) the BSA/$Ru(bpy)_3^{2+}$-bilayer-coated ITO electrode, and (3) a bare ITO electrode. Conditions are as for Figure 2A. For comparison, the spectra of (1) and (2) were scaled up 15 and 2 times, respectively.

brings $Ru(bpy)_3^{2+}$ to the vicinity of the electrode surface and, more importantly, the much faster electron-transfer rate of $Ru(bpy)_3^{2+}$ in the bilayer, which minimizes the effect of electron tunneling across the underlying insulating BSA monolayer and effectively mediates charge transfer between oxalate and the ITO electrode.[25,26] Clearly, these results indicate that the observed photocurrent of the system appears to be due principally to the photoelectrochemical response of oxalate at the ITO electrode although a photosensitizing tag is present at the bilayer-coated electrode. The fact that the respective photocurrent action spectrum remained essentially unchanged after coating with the bilayer suggests that $Ru(bpy)_3^{2+}$ itself has little if any photoelectrochemical response in the system. The decrease in photocurrent observed at the bilayer-coated electrode is due to the presence of the BSA film, although its blocking effect is largely overcome by $Ru(bpy)_3^{2+}$. At the moment we cannot totally rule out some small contribution from $Ru(bpy)_3^{2+}$. However, the main contribution of the photocurrent is from oxalate.

Conclusions

In summary, the photoelectrochemical response of oxalate was observed at the bare ITO electrode. It was found that the photocurrent is dependent on the concentration of oxalate, illumination wavelength, incident light intensity, and applied potential. While photoelectrochemical responses of the $Ru(bpy)_3^{2+}$−oxalate system have been shown, with enhanced photocurrent in comparison with a control electrode,[10] a similar photocurrent was also seen at the bare ITO electrode. We emphasize the need for caution in attributing photoelectrochemical properties to $Ru(bpy)_3^{2+}$ without conducting the appropriate control experiments. The "photosensitizing effect" of $Ru(bpy)_3^{2+}$ seen in the $Ru(bpy)_3^{2+}$−oxalate system is more a "mediating" effect due to its fast electrode kinetics. It is interesting to speculate that the presence of $Ru(bpy)_3^{2+}$ at the ITO surface may actually improve the performance of the photoelectrochemical response by introducing the photosensitizing $Ru(bpy)_3^{2+}$ and blocking access of interfering species to the electrode surface, while the photoelectrochemical response to oxalate through the BSA monolayer could still take place. In any event, these results indicate that the development of photoelectroanalytical systems must take into account the properties of the substrate materials and the sacrificial electron

donor/acceptor employed in their construction. Caution is, therefore, suggested in the development of photoelectrochemistry-based analytical techniques.

Acknowledgment. We acknowledge financial support from IBN/A*STAR.

References and Notes

(1) Hagfeldt, A.; Grätzel, M. *Chem. Rev.* **1995**, *95*, 49.
(2) Grätzel, M. *Heterogeneous Photochemical Electron Transfer*; CRC Press: Boca Raton, FL, 1989.
(3) Bard, A. J.; Fox, M. A. *Acc. Chem. Res.* **1995**, *28*, 141.
(4) Hotchandani, S.; Kamat, P. V. *Chem. Phys. Lett.* **1992**, *191*, 320.
(5) Liu, D.; Kamat, P. V. *J. Electrochem. Soc.* **1995**, *142*, 835.
(6) O'Regan, B.; Grätzel, M. *Nature* **1991**, *353*, 737.
(7) Nazeeruddin, M.; Kay, A.; Rodicio, I.; Humphry-Baker, R.; Muller, E.; Liska, P.; Vlachopoulos, N.; Grätzel, M. *J. Am. Chem. Soc.* **1993**, *115*, 6382.
(8) Li, W.; Osora, H.; Otero, L.; Duncan, D. C.; Fox, M. A. *J. Phys. Chem. B* **1998**, *102*, 5333.
(9) Konishi, T.; Ikeda, A.; Asai. M.; Hatano, T.; Shinkai, S.; Fujitsuka, M.; Ito, O.; Tsuchiya. Y.; Kikuchi. J. *J. Phys. Chem. B* **2003**, *107*, 11261.
(10) Dong, D.; Zheng, D.; Wang, F.; Yang, X.; Wang, N.; Li, Y.; Guo, L.; Cheng, J. *Anal. Chem.* **2004**, *76*, 499.
(11) Nakamura, S.; Shibata, A.; Takenaka, S.; Takagi, M. *Anal. Sci.* **2001**, *17*, i431.
(12) Calvert, J. G.; Pitts, J. N. *Photochemistry*; John Wiley: New York, 1973.
(13) Bedja, I.; Hotchandani, S.; Kamat, P. V. *J. Phys. Chem.* **1994**, *98*, 4133.
(14) Sodergren, S.; Hagfeldt, A.; Olsson, J.; Lindquist, S.-E. *J. Phys. Chem.* **1994**, *98*, 5552.
(15) Schwarzburg, K.; Willig, F. *Appl. Phys. Lett.* **1991**, *58*, 2520.
(16) Hasobe, T.; Imahori, H.; Fukuzumi, S.; Kamat, P. V. *J. Phys. Chem. B* **2003**, *107*, 12105.
(17) Suarez, R.; Nair, P. K.; Kamat, P. V. *Langmuir* **1998**, *14*, 3236.
(18) Segui, J.; Hotchandani, S.; Baddou, D.; Leblanc, R. M. *J. Phys. Chem.* **1992**, *95*, 8807.
(19) (a) Kavan, L.; O'Regan, B.; Kay, A.; Gratzel, M. *J. Electroanal. Chem.* **1993**, *346*, 291. (b) O'Regan, B.; Moser, J.; Anderson, M.; Grätzel, M. *J. Phys. Chem.* **1990**, *94*, 8720.
(20) Bedja, I.; Kamat, P. V.; Hua, X.; Lappin, A. G.; Hotchandani, S. *Langmuir* **1997**, *13*, 2398.
(21) Salvador, P. *J. Phys. Chem.* **1985**, *89*, 3863.
(22) Lvov, Y.; Lu, Z.; Schenkman, T. B.; Zu, X.; Rusling, J. F. *J. Am. Chem. Soc.* **1998**, *120*, 4073.
(23) Ulman, A. *An Introduction to Ultrathin Organic Films From Langmuir Blodgett to Self-Assembly*; Academic Press: San Diego, CA, 1991.
(24) Decher, G. *Science* **1997**, *277*, 1231.
(25) Xie, H.; Yu, Y. H.; Mao, P.; Gao, Z. *Nucleic Acids Res.* **2004**, *32*, e15.
(26) Xie, H.; Zhang, C.; Gao, Z. *Anal. Chem.* **2004**, *76*, 1161.